HHS Public Access

Author manuscript

Ophthalmic Surg Lasers Imaging Retina. Author manuscript; available in PMC 2016 January 14.

Published in final edited form as:

Ophthalmic Surg Lasers Imaging Retina. 2014 ; 45(5): 459–461. doi:10.3928/23258160-20140909-01.

Spectral-Domain and Swept-Source OCT Imaging of Asteroid Hyalosis: A Case Report

Tarek Alasil, MD, **Mehreen Adhi, MD**, **Jonathan J. Liu, PhD**, **James G. Fujimoto, PhD**, **Jay S. Duker, MD**, and **Caroline R. Baumal, MD**

New England Eye Center (TA, MA, JSD, CRB), Tufts Medical Center, Boston, Massachusetts; and the Department of Electrical Engineering and Research Laboratory of Electronics (JJL, JGF), Massachusetts Institute of Technology, Cambridge, Massachusetts

Abstract

A 72-year-old man with diabetes was referred to the retina clinic for diabetic retinopathy. Detailed funduscopic examination of the left eye was limited by prominent asteroid hyalosis. Spectral-domain (SD) and swept-source (SS) optical coherence tomography (OCT) were utilized to examine the vitreous, vitreoretinal interface, and the morphology of the retina. Asteroid hyalosis induced artifacts of the OCT images, which resolved when the appropriate imaging protocols were applied. SS-OCT may show superior diagnostic and preoperative capabilities when compared to SD-OCT in the settings of asteroid hyalosis-induced media opacity.

INTRODUCTION

Asteroid hyalosis is a degenerative process of the vitreous resulting in the formation of small white opacities, which consist of calcium phosphate and lipid deposits.[1] Asteroid hyalosis rarely impairs visual acuity, but it can limit fundus visualization because of the scattered reflection of light off the asteroid opacities.[1]

Hwang et al[2] demonstrated the clinical utility of time-domain optical coherence tomography (TD-OCT) in diagnosing macular structural abnormalities when retinal visualization was limited by asteroid hyalosis. Mochizuki et al[3] investigated the anatomical features of vitreoretinal interface in 10 eyes with asteroid hyalosis by comparing the findings during vitrectomy to the preoperative TD-OCT images. The posterior vitreous cortex could not be clearly identified with preoperative TD-OCT in two of 10 eyes. However, a complete posterior vitreous detachment was ruled out intraoperatively in those two eyes after visualization of the posterior vitreous cortex with triamcinolone acetonide.

We present a case report of spectral-domain (SD) and swept-source (SS) OCT imaging of asteroid hyalosis.

Address correspondence to Caroline R. Baumal, MD, New England Eye Center, Tufts Medical Center, 260 Tremont Street, Boston, MA 02116; 617-636-7950; fax: 617-636-4866; cbaumal@gmail.com.

The authors have no financial or proprietary interest in the materials presented herein.

Dr. Duker did not participate in the editorial review of this manuscript.

CASE REPORT

A 72-year-old man with diabetes was referred for retina evaluation. He had a history of diabetic macular edema for which he had received focal laser bilaterally. He had proliferative diabetic retinopathy (PDR), which was quiescent after panretinal photocoagulation.

Best corrected visual acuity was counting fingers in the right eye and 20/30 in the left. Posterior segment examination in the right eye revealed previous focal laser and panretinal photocoagulation. There was no active macular edema. Funduscopic examination of the left macular details was limited by prominent asteroid hyalosis (Figure 1A). Cirrus HD-OCT (Carl Zeiss Meditec, Dublin, CA) revealed the presence of vitreomacular adhesion, and there was no macular edema in the left eye (Figures 1B–C). Enhanced depth imaging (EDI) was applied as well (Figure 1D).

Multiple wide-field scans (500 A-scans × 500 B-scans over 12 × 12 mm) were obtained using a prototype long-wavelength SS-OCT system in the left eye. A motion correction algorithm was applied to merge the scans into a single volumetric data set.[4] The improved signal and image contrast further delineated the asteroid hyalosis within the vitreous as well as the retinal structures underneath (Figures 2A and 2C). The 3D-imaging clearly demonstrated vitreomacular adhesions with vitreoschisis (Figures 2B and 2D).

DISCUSSION

The vitreous is a highly hydrated gel-like substance that provides structural support to the globe while serving as a clear unobstructed pathway for light to reach the retina. The most common clinically observed degenerative opacity of vitreous is asteroid hyalosis.

In our case, standard Cirrus OCT imaging of asteroid hyalosis showed multiple axially stretched and blurred hyperreflective spots within the vitreous and underneath the choroid (Figures 1B and 1C). These artifacts occurred because the asteroid bodies were positioned on the other side of the zero delay from the retina when the images were acquired.[5] Therefore, mirror artifacts of the asteroid bodies were generated within the OCT image range and were observed as blurred artifacts above the retina (Figure 1B) and beneath the choroid (Figure 1C). These artifacts were corrected with EDI imaging (Figure 1D).[6] Furthermore, we noted multiple hyperreflective granules within the vitreous and underneath the choroid by using SS-OCT (Figures 2A–B). Those artifacts were absent when the device was pushed close enough to the eye to create an inverted image near the top of the display in order to correct for the mirror effect (Figures 2C–D). Artifact-free imaging demonstrated that the asteroid bodies were further away from the retina (Figure 2D) than they seem in a non-flipped image (Figure 2B). This case demonstrates that the EDI setting on the Cirrus SD-OCT was equivalent to setting the zero delay posterior to the retina and inverting the image on the SS-OCT in order to overcome mirror artifacts. This highlights the importance of understanding the technology to image patients with appropriate protocols using SD- and SS-OCT, in order to minimize artifacts and visualize the true topography of the posterior eye. It is not possible to apply EDI to the 3D rendering on the commercial Cirrus HD-OCT,

whereas 3D artifact-free imaging is possible with the SS-OCT prototype (Figures 1C and 2D).

We report the potential clinical advantages of visualizing the vitreoretinal interface by using the longer axial imaging range provided by SS-OCT in patients with PDR despite the presence of asteroid hyalosis. Patients with PDR may experience different complications that require intervention from vitreoretinal surgeons. Clear wide-field preoperative demonstration of the vitreoretinal interface in those patients may provide the advantage of making the surgery more smooth and the outcome more predictable. In our case, SS-OCT clearly demonstrated vitreomacular adhesions with vitreoschisis, whereas SD-OCT suggested vitreomacular adhesions with no macular edema. Further studies are warranted to prove this SS-OCT potential advantages in cases with severe asteroid hyalosis and vitreous abnormalities.

It has been established that substances can diffuse from the degenerating retina into the vitreous. Irish setters with hereditary rod-cone dysplasia have been reported to have active lipid metabolism in the vitreous.[7] Furthermore, asteroid hyalosis has been reported in patients with retinitis pigmentosa[8] or pigmentary retinal degeneration.[9] SS-OCT might provide an in vivo tool to better understand the pathophysiology of asteroid body formation in these retinal diseases, because SS-OCT has the advantage of providing long-wavelength, motion-corrected, artifact-free 3D visualization of the posterior vitreous and the vitreoretinal interface over a 12 × 12 mm wide field of view (two times wider than 6 × 6 mm provided by Cirrus OCT). Therefore, SS-OCT may show superior diagnostic and preoperative capabilities when compared to SD-OCT in those patients with asteroid hyalosis.

In conclusion, SS-OCT has the advantage of providing long-wavelength, motion-corrected, artifact-free 3D visualization of the posterior vitreous and the vitreoretinal interface over a wide field of view and long imaging range. SS-OCT may show superior diagnostic and preoperative capabilities when compared to SD-OCT in patients with asteroid hyalosis.

Acknowledgments

Supported in part by National Institute of Health (NIH) contracts R01-EY11289-27 and R01-EY13178-12; Air Force Office of Scientific Research FA9550-10-1-0551, FA9550-12-1-0499; German Research Foundation (DFG) DFG-HO-1791/11-1, DFG Research Training Group 1773, and DFG-GSC80-SAOT; the Massachusetts Lions Club; and a Research to Prevent Blindness unrestricted grant to the New England Eye Center. The sponsors or funding organizations had no role in the design or conduct of this research.

The authors gratefully acknowledge Martin Kraus, Dr. Ireneusz Grulkowski, Chen Lu, WooJhon Choi, Dr. Benjamin Potsaid, and Dr. Joachim Hornegger for their scientific contributions.

REFERENCES

1. Fawzi AA, Vo B, Kriwanek R, et al. Asteroid hyalosis in an autopsy population: The University of California at Los Angeles (UCLA) experience. Arch Ophthalmol. 2005; 123(4):486–490. [PubMed: 15824221]
2. Hwang JC, Barile GR, Schiff WM, et al. Optical coherence tomography in asteroid hyalosis. Retina. 2006; 26(6):661–665. [PubMed: 16829809]

3. Mochizuki Y, Hata Y, Kita T, et al. Anatomical findings of vitreoretinal interface in eyes with asteroid hyalosis. Graefes Arch Clin Exp Ophthalmol. 2009; 247(9):1173–1177. [PubMed: 19421766]
4. Kraus MF, Potsaid B, Mayer MA, et al. Motion correction in optical coherence tomography volumes on a per A-scan basis using orthogonal scan patterns. Biomed Opt Express. 2012; 3(6): 1182–1199. [PubMed: 22741067]
5. Ho J, Castro DP, Castro LC, et al. Clinical assessment of mirror artifacts in spectral-domain optical coherence tomography. Invest Ophthalmol Vis Sci. 2010; 51(7):3714–3720. [PubMed: 20181840]
6. Spaide RF, Koizumi H, Pozoni MC. Enhanced depth imaging spectral-domain optical coherence tomography. Am J Ophthalmol. 2008; 146(4):496–500. [PubMed: 18639219]
7. Reddy TS, Birkle DL, Packer AJ, Dobard P, Bazan NG. Fatty acid composition and arachidonic acid metabolism in vitreous lipids from canine and human eyes. Curr Eye Res. 1986; 5(6):441–447. [PubMed: 3089690]
8. van den Born LI, van Soest S, van Schooneveld MJ, et al. Autosomal recessive retinitis pigmentosa with preserved para-arteriolar retinal pigment epithelium. Am J Ophthalmol. 1994; 118(4):430–439. [PubMed: 7943119]
9. Sebag J, Albert DM, Craft JL. The Alstrom syndrome: ophthalmic histopathology and retinal ultrastructure. Br J Ophthalmol. 1984; 68(7):494–501. [PubMed: 6733075]

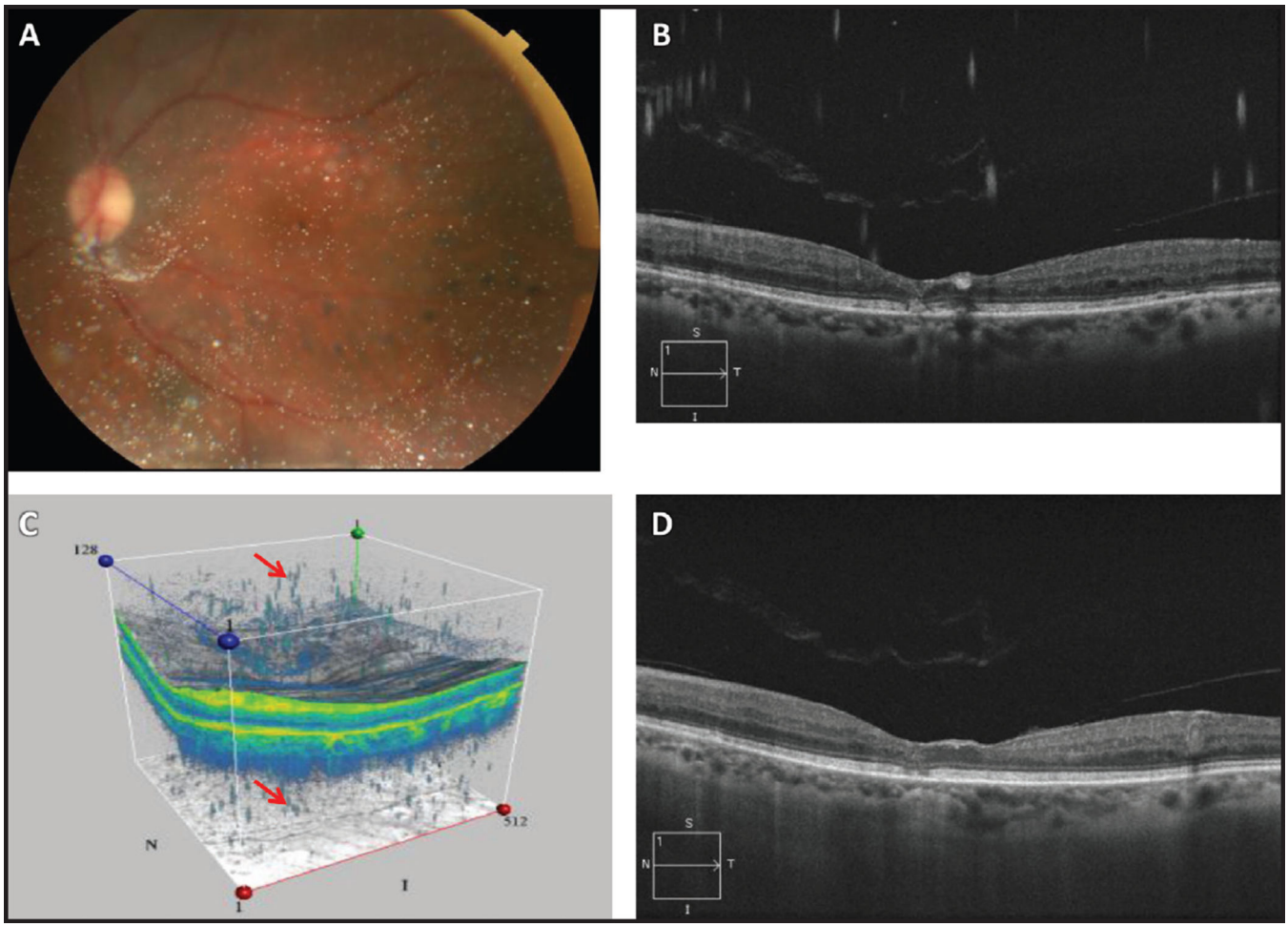

Figure 1.

Asteroid hyalosis (AH). (A) Fundus photograph of the left eye reveals AH. (B) Cirrus HD-OCT image shows multiple artifacts around the AH. (C) Cirrus HD-OCT 3D image shows multiple artifacts around AH and more artifacts beneath the choroid (arrows). (D) Cirrus HD-OCT one-line raster enhanced depth image demonstrates vitreomacular adhesion with no artifacts.

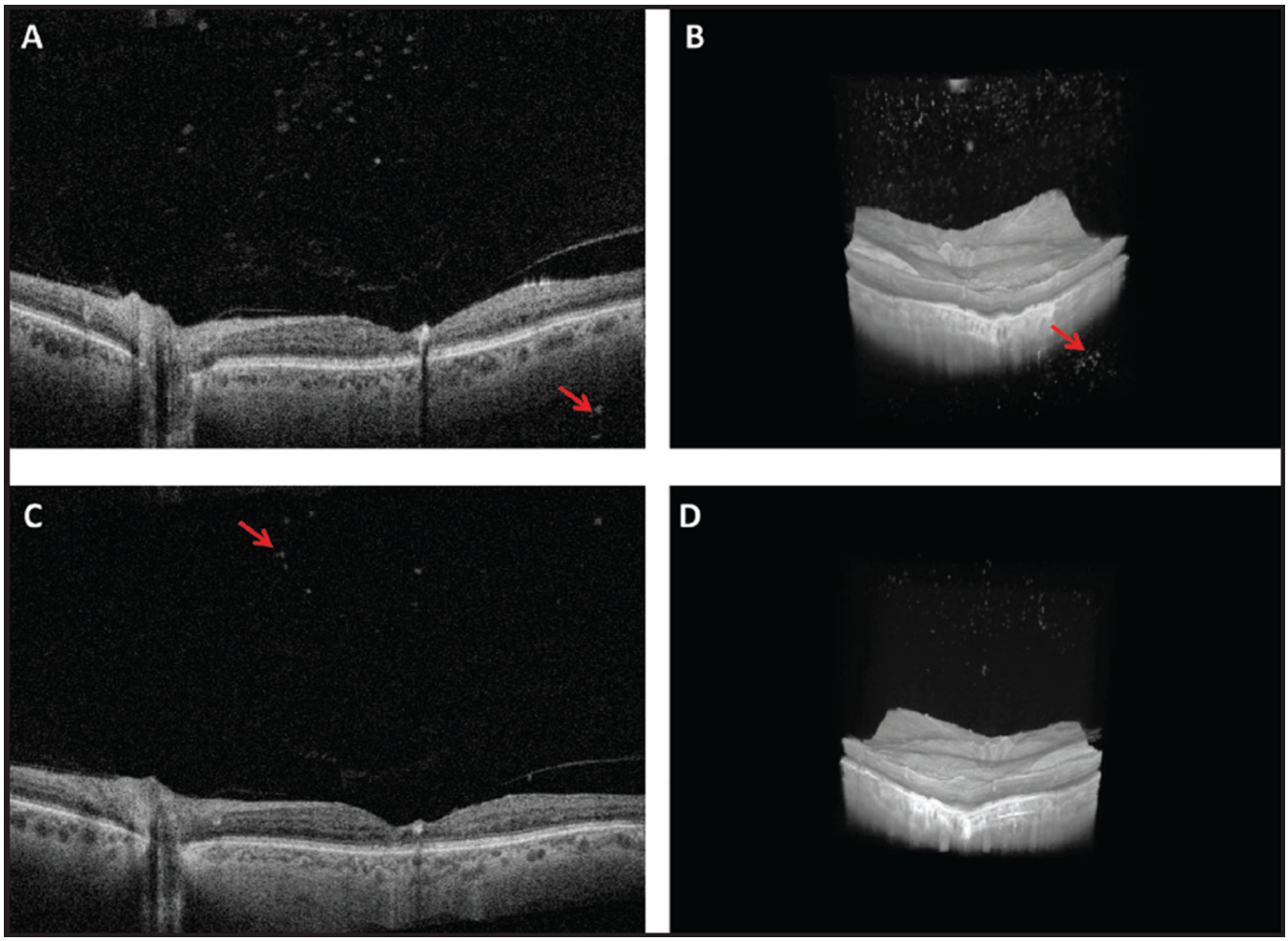

Figure 2.

(A) Wide-field swept-source OCT cross-sectional image shows vitreomacular adhesion, asteroid hyalosis (AH), and artifacts beneath the choroid (arrow). (B) Swept-source OCT 3D image shows vitreomacular adhesion, vitreoschisis, and AH with artifacts beneath the choroid (arrow). (C) Wide-field swept-source OCT cross-sectional flipped image shows vitreomacular adhesion and artifact-free AH (arrow). (D) Swept-source OCT 3D flipped image shows vitreomacular adhesion, vitreoschisis, and artifact-free AH.